Synthesis, Bioactivity Assessment, and Molecular Docking of Non-sulfonamide Benzimidazole-Derived *N*-Acylhydrazone Scaffolds as Carbonic Anhydrase-II Inhibitors

Muhammad Saadiq,* Ghias Uddin,* Abdul Latif, Mumtaz Ali, Nazia Akbar, Ammara, Sardar Ali, Manzoor Ahmad, Mohammad Zahoor, Ajmal Khan, and Ahmed Al-Harrasi

Read Online

ACCESS | Metrics & More | Article Recommendations
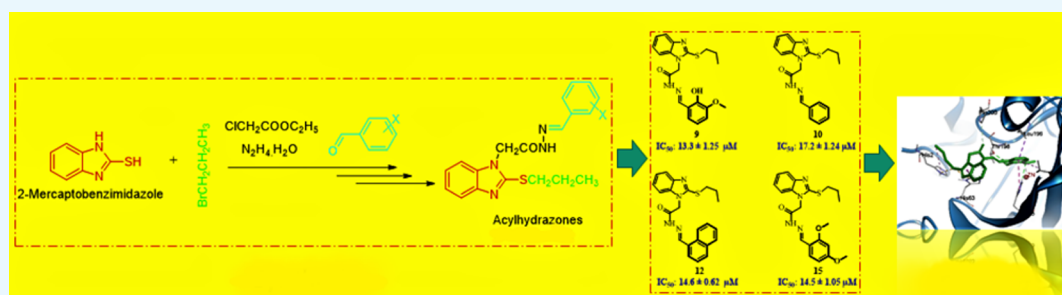
ABSTRACT: This research reports the synthesis of new benzimidazole-derived *N*-acylhydrazones (NAH), their characterization using various spectroscopic methods, and in vitro evaluation as potent carbonic anhydrase-II inhibitors. Among the target compounds (**9−29**), few showed higher inhibition than the standard acetazolamide (IC$_{50}$: 18.6 ± 0.43 μM), for example, compound **9** (IC$_{50}$: 13.3 ± 1.25 μM), **10** (IC$_{50}$: 17.2 ± 1.24 μM), **12** (IC$_{50}$: 14.6 ± 0.62 μM), and **15** (IC$_{50}$: 14.5 ± 1.05 μM). Molecular docking was performed on the most active compounds, which revealed their binding interactions with the active site of the enzyme, thus supporting the experimental findings.

INTRODUCTION

Carbonic anhydrases (CAs) are zinc-containing enzymes that catalyze the reversible hydration of carbon dioxide to bicarbonate ions and protons. They are involved in a wide range of physiological processes, such as pH regulation, gas exchange, ion transport, bone resorption, fatty acid metabolism, and so forth. Their abnormal levels result in glaucoma and edema. Many CA inhibitors (CAIs) mostly belong to the sulfonamide class such as benzimidazole-6-sulfonamides, acetazolamide, methazolamide, ethoxzolamide, dichlorophenamide, benzenesulfonamide, and so forth.[1−4]

However, numerous sulfonamides inhibit all CA isoforms non-specifically, causing undesired side effects and reducing drug effectiveness owing to off-target inhibition. Furthermore, due to sulfa allergy, a substantial percentage of the general population cannot be treated with sulphonamides; consequently, non-sulphonamide-based CAIs must be developed.[5]

Benzimidazole is a privileged chemical scaffold with tremendous biological applications. Some of the benzimidazole-based market drugs are omeprazole, pantoprazole (proton pump inhibitor), triclabendazole, thiabendazole, albendazole (anthelmintic), benomyl, carbendazim, fuberidazole (fungicide), candesertan, telmisartan (anti-hypertensive), mebenda-

zole (worm infestation), astemizole (antihistamine), bendamustine (anti-cancer), afobazole (anxiolytic), casein kinase-1 inhibitors, pan RAF kinase inhibitors, and so forth.[6−9]

Benzimidazole-2-thiol (B2T) is an important derivative of benzimidazole with potential bioactivities. For example, a series of amide derivatives based on B2T has been reported with antimicrobial activity against *Candida albicans*, *Staphylococcus aureus*, and *Escherichia coli*.[10] Another research study revealed high anti-convulsant activity for B2T derivatives.[11] A pharmacophore consisting of α-bromophenyallylidene on B2T imines has been shown to enhance antimicrobial and antiproliferative activities.[12] A variety of structural forms based on B2T with medicinal applications include acyclic nucleosides as antibacterial agents,[13] aminoacetylenic-5-ethoxy-2-mercaptobenzimidazoles as antibacterial and antifungal agents,[14] 2-MBI incorporated with thiazolidinone and

Scheme 1. Synthetic Route Leading to Benzimidazole-Derived *N*-Acylhydrazones (9−29)

Reaction conditions:
a. KOH/EtOH-reflux   b. DMF, Na$_2$CO$_3$-reflux
c. MeOH-reflux   d. MeOH, AcOH-reflux

Substituent- X:

X = 8a

9). 2-OH, 3-OCH$_3$	10). Ph
11). 3-OCH$_3$	12). Naphthyl-
13). 3,4-OCH$_3$	14). 2,4-OH
15). 2,4-OCH$_3$	16). 4-N(CH$_2$CH$_3$)$_2$
17). 3-OH	18). 4-OH, 3-OCH$_3$
19). 4-CH$_3$	20). 3-OCH$_2$CH$_3$, -4-OH
21). 4-CHO	22). (CH$_3$)$_2$CH-
24). 4-F	27). 2,3-OCH$_3$
28). 2,6-Cl	29). 2-OCH$_3$

X = 8b

23). 2-Thiophene	25). 2-Furan
26). 5-methylfuran	
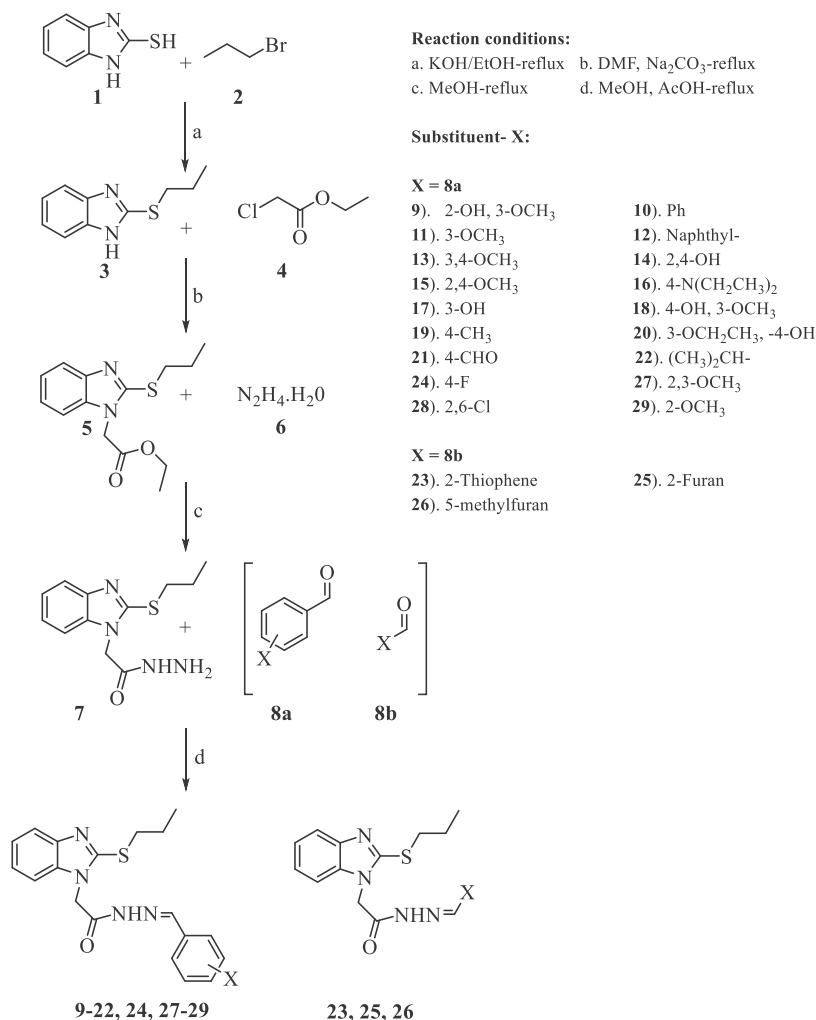
isoxazole heterocycles as potent anticonvulsant and anti-inflammatory/analgesic agents,[15] 2-MBI triazolylacetohydrazides as antimicrobial, anti-inflammatory and analgesic agents,[16] afobazole as a potent anxiolytic drug,[17] and B2T oxadiazoles as antidiabetic agents.[18]

Benzimidazole-2-thiol-based *N*-acylhydrazones have been reported as an antioxidant and α-glucosidase and cholinesterase inhibitors.[19,20] These findings laid the base to investigate the benzimidazole-derived *N*-acylhydrazones for carbonic anhydrase inhibitory potential.

Molecular docking is a computational technique that attempts to predict the binding of small molecules and large/macromolecules (receptor) efficiently starting with their unbound structures. This procedure is used not only to anticipate whether a ligand binds tightly to the target but also to understand how it binds. To study the mechanism of inhibition for carbonic anhydrase-II and the binding modes of acylhydrazones (9−29), molecular docking studies were performed. Bovine carbonic anhydrase-II (PDB ID: 1V9E) in complex with zinc metal was downloaded from the Protein Data Bank and used for docking of compounds.[21,22] The active site of carbonic anhydrase-II where zinc metal is present lies at the bottom of the deep cleft. The ligand−receptor interactions and binding modes in the binding cavity of bovine carbonic anhydrase-II in 2D and 3D forms were examined carefully by visual evaluation employing GOLD. The docked orientation of

compounds showed the direct interaction of the zinc ion present in the active gorge and the ligand.

■ RESULTS AND DISCUSSION

Chemistry. A multi-step reaction pathway leads to the synthesis of *N*-acylhydrazones. In the first step, benzimidazole-2-thiol (**1**) was alkylated with *n*-bromopropane (**2**) in absolute ethanol to yield 2-(propylthio)benzimidazole (**3**). Then, the *N*-alkylation of 2-(propylthio)benzimidazole was carried out using chloroethylacetate (**4**) in DMF to get 2-(2-propylthio)-benzimidazolyl)acetate (**5**). In the third step, compound **5** was substituted with hydrazine hydrate (**6**), resulting in the corresponding acetohydrazide (**7**). Condensation of compound **7** with different aldehydes (**8a,b**) yielded a series of *N*-acylhydrazones (**9−29**). Purity of the synthesized compounds was monitored by TLC in *n*-hexane and ethyl acetate solvent systems and observed under UV light. The structures of all compounds (Scheme 1) were determined with the help of different spectroscopic techniques such as ^{1}H NMR, ^{13}C NMR, and HR-MS(ESI). The main features of the final products (**9−29**) in their ^{1}H NMR spectra included protons of the thiopropyl group (−SC$_3$H$_7$) at δ 0.95−3.30, methylene protons (−NCH$_2$CO−) at δ 5.31−5.76, amide protons (−CO−NH−) at δ 11.47−12.09, imine protons (−N═CH−) at δ 7.90−8.77 ppm, and aromatic protons of the

benzimidazole nucleus and different aromatic aldehydes in the aromatic region of the spectrum and other substituents ,OH, CH_3, OCH_3, and $N(CH_2CH_3)$, and so forth at the imine displaying varying chemical shift values. The ESI-MS of the products displayed molecular ion peak $(M + H)^+$ characteristics of the compounds. After confirmation of structures of the compounds, they were evaluated in vitro against the bovine carbonic anhydrase-II enzyme. The inhibition profile is presented in Table 1, and the probable mechanism of inhibition was studied through molecular docking represented in Figures 2–6.

Table 1. In Vitro Carbonic Anhydrase Inhibition Potential of 9−29[a,b]

comp. no.	% inhibition	IC$_{50}$ ± S.E.M (μM)
9	89.1	13.3 ± 1.25
10	83.0	17.2 ± 1.24
11	22.8	NA
12	91.7	14.6 ± 0.62
13	38.1	NA
14	20.8	NA
15	91.2	14.5 ± 1.05
16	5.6	NA
17	90.7	31.4 ± 2.29
18	81.2	22.7 ± 1.37
19	13.6	NA
20	67.7	45.5 ± 2.07
21	42.2	NA
22	90.1	24.7 ± 3.00
23	89.8	24.8 ± 1.24
24	84.3	162.3 ± 3.54
25	57.0	193.5 ± 3.24
26	67.8	166.0 ± 1.61
27	89.6	55.6 ± 4.25
28	67.6	42.1 ± 1.39
29	88.2	21.0 ± 0.74
acetazolamide	86.7	18.6 ± 0.43

[a]S.E.M: standard error of mean. [b]NA: not active.

Carbonic Anhydrase Inhibition Activity. In vitro carbonic anhydrase inhibition activity of the target compounds (9−29) was evaluated using reported methods.[21] All the target compounds showed inhibition activity against bCA-II except 11, 13, 14, 16, 19, and 21, which were found inactive (Table 1). Furthermore, compounds 10, 12, 15, and 9 showed higher inhibitions than the standard **acetazolamide** (IC$_{50}$: 18.6 ± 0.43 μM) where compound 9 was the most active inhibitor (IC$_{50}$: 13.3 ± 1.25 μM) followed by 15 (IC$_{50}$: 4.5 ± 1.05 μM), 12 (IC$_{50}$: 14.6 ± 0.62 μM), and 10 (IC$_{50}$: 17.2 ± 1.24 μM). However, compounds 23 (IC$_{50}$: 24.8 ± 1.24 μM), 22 (IC$_{50}$: 24.7 ± 3.00 μM), 18 (IC$_{50}$: 22.7 ± 1.37 μM), and 29 (IC$_{50}$: 21.0 ± 0.74 μM) showed comparable inhibition to the standard, while compounds 17, 20, 24, 25, 26, 27, and 28 were found to be the least active inhibitors of the enzyme.

Figure 1 displays the most active inhibitors (9, 10, 12, and 15), highlighting the substituents (−2-OH, 3-OCH$_3$, −Ph, −naphthalene, and −2,4-OCH$_3$) on the benzylidene ring, which imparted them effective inhibition ability. A comparison of the activity of compound 9 with compounds 10, 12, and 15 reveals the importance of 2-OH and 2-CH$_3$ groups in the inhibition potential against bCA-II. Similarly, the presence of −2,4-OCH$_3$ groups on the benzene ring of compound 15

9
IC$_{50}$: 13.3 ± 1.25 μM

10
IC$_{50}$: 17.2 ± 1.24 μM

12
IC$_{50}$: 14.6 ± 0.62 μM

15
IC$_{50}$: 14.5 ± 1.05 μM

Substituents activating the bCA-II potential
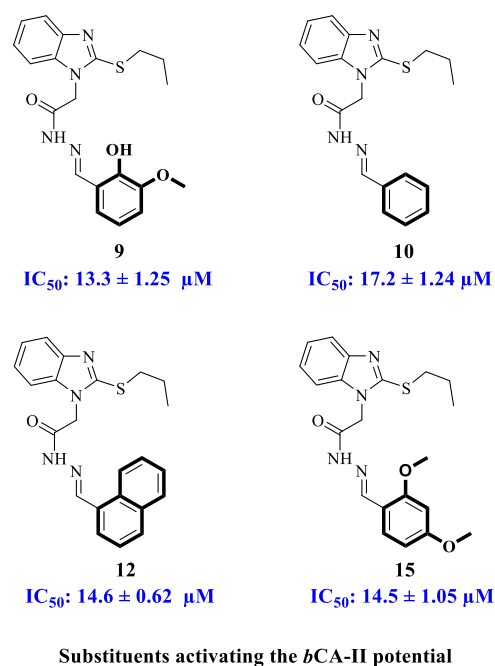
Figure 1. Structures of the most active inhibitors 9, 10, 12, and 15.

makes it a comparably stronger inhibitor of CA. The present study reports non-sulfonamide carbonic anhydrase II inhibitors by incorporating the benzimidazole and N-acylhydrazone scaffolds in a single nucleus.

Molecular Docking. To examine the interaction of the ligand with the active site of the receptor, four most active compounds (9, 10, 12, and 15) were modeled. For comparison, the standard acetazolamide (yellow stick model) was also docked (GOLD fitness score of 48.2) in the Zn^{+2} bound cavity of 1V9E (Figure 2). Important interactions observed were of metal−acceptor (Zn), H-bonding (His95, His93, His63, His118, Thr198, Thr197, and Gln91), and Pi−sulfur (His63, His93, and His95).
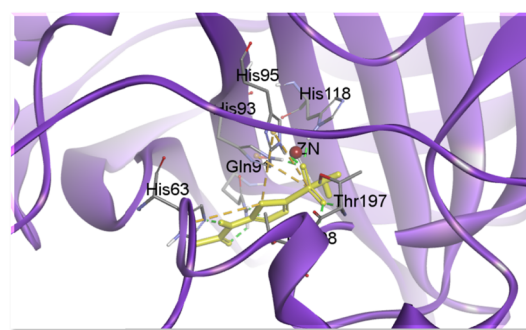
Figure 2. Close-up view of the top-scoring pose of acetazolamide (yellow stick model) showing detailed ligand−enzyme interactions.

Compound 9 was found to be the most active, showing interactions with different amino acid residues and having a GOLD fitness score of 52.5. The aromatic ring was predicted to have π−π T-shaped, π−sigma, and π−alkyl interactions with His93, leu98, and Val120, respectively. The thiopropyl chain showed π−alkyl, π−sigma, and π−π T-shaped interactions with His2 and His63. Metal−acceptor interactions with ZN260, carbon−hydrogen bonding with Pro200, and hydrogen bonding were also witnessed with Thr198 (Figure 3).
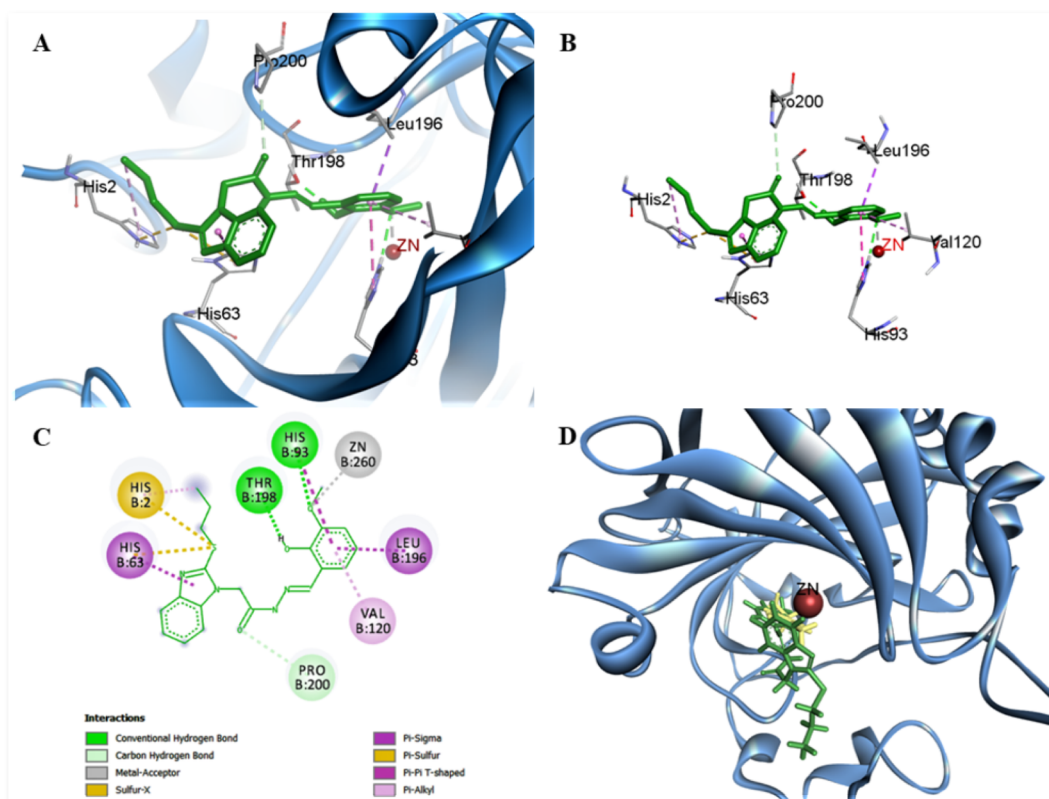
Figure 3. (A) Close-up view of the top-scoring pose of compound **9** (green stick model) showing detailed ligand−enzyme interactions; (B) stereoview of ligand−enzyme interactions; (C) 2D view of ligand−enzyme interactions; and (D) compound **9** (green stick model) superimposed on acetazolamide (yellow stick model), the active site.

Compound **10**, another active compound among the series, displayed interactions with amino acid residues of the active site, having a GOLD score of 51.7. The important amino acid residues involved in these interactions are Thr198, Thr197, Leu196, Val141, Val120, His93, His63, and Val59. The interactions predicted for the aromatic ring include π−alkyl with Val120 and Val121, π−sigma with Leu196, π−π T-shaped with His93, π−donor hydrogen bond with Thr197, and π−cation with ZN260. Thr198 exhibited H-bonding with the nitrogen atom of the imine functional group. Val59 displayed alkyl interactions with the CH_3 group of the thiopropyl chain. Aromatic rings of the mercaptobenzimidazole nucleus were predicted to involve π−sigma and π−π T-shaped interactions with His63 (Figure 4).

Compound **12** with a GOLD fitness score of 52.1 occupied the active gorge of 1V9E with a pose similar to that of acetazolamide. Among important interactions of the aromatic rings, π−donor H-bonding with TRp4 and Thr197 residues is included. His93, Val120, Leu196, Thr197, Pro200, and ZN260 displayed π−π T-shaped, π−alkyl, π−sigma, π−donor H-bonding, π−alkyl, and π−cation interactions with aromatic rings. His2 demonstrated π−alkyl interactions with the alkyl group (Figure 5).

The GOLD score of compound **15** was calculated as 53.0, showing a very good fit in the binding cavity of the enzyme having a Zn^{+2} ion. Upon visual inspection, some important interactions of the ligand and amino acid residues can be seen. Zn260, Thr197, and His95 were witnessed for their metal−acceptor and hydrogen bonding interactions with compound **15**. The π−sigma interaction was predicted for Thr198 and His93 with the aromatic ring and methoxy group. Similarly, the

phenyl ring showed π−alkyl interactions with Leu196. His2 and Trp4 exhibited π−π T-shaped and π−donor H-bonding with the aromatic ring of the mercaptobenzimidazole nucleus (Figure 6).

EXPERIMENTAL SECTION

Chemistry. Chemicals were purchased from BDH, Daejung, Alfa Aesar, Merck, and Aldrich. Melting points were determined on Gallenkamp digital melting point equipment MGB-595-010 M. Silica gel plates (Aldrich) were employed for TLC. The ^1H NMR and ^{13}C NMR spectra were recorded on a Bruker AVANCE spectrometer (600 and 150 MHz, made in Germany)/DMSO with TMS as an internal standard. The HR-MS(ESI) was recorded on a JEOL JMS600. The chemical synthesis given below was performed according to the reported methods.[19,20]

Synthesis of 2-(Propylthio)-1*H*-benzo[*d*]imidazole (3). A total of 133 mmol (20 g) 2-MBI (**1**) was taken in an RB flask in 40 mL of ethanol, to which 133 mmol (7.5 g) KOH was added and heated over a magnetic hotplate stirrer. Then, 133 mmol (12 mL) bromopropane (**2**) was added. After completion, the reaction mixture was filtered and dried to get white needle-like crystals of the product.

Synthesis of Ethyl 2-(2-(Propylthio)-1*H*-benzo[*d*]-imidazol-1-yl)acetate (5). A total of 80 mmol 2-propylth-iobenzimidazole (15.45 g) (**3**) was taken in an RB flask in DMF, to which 80 mmol K_2CO_3 (11.05 g) was added. Then, 80 mmol chloroethylacetate (**4**) (9.8 mL) was added dropwise and refluxed at 100 °C for 12 h. After completion, the product was extracted in an ethyl acetate−water system and dried.
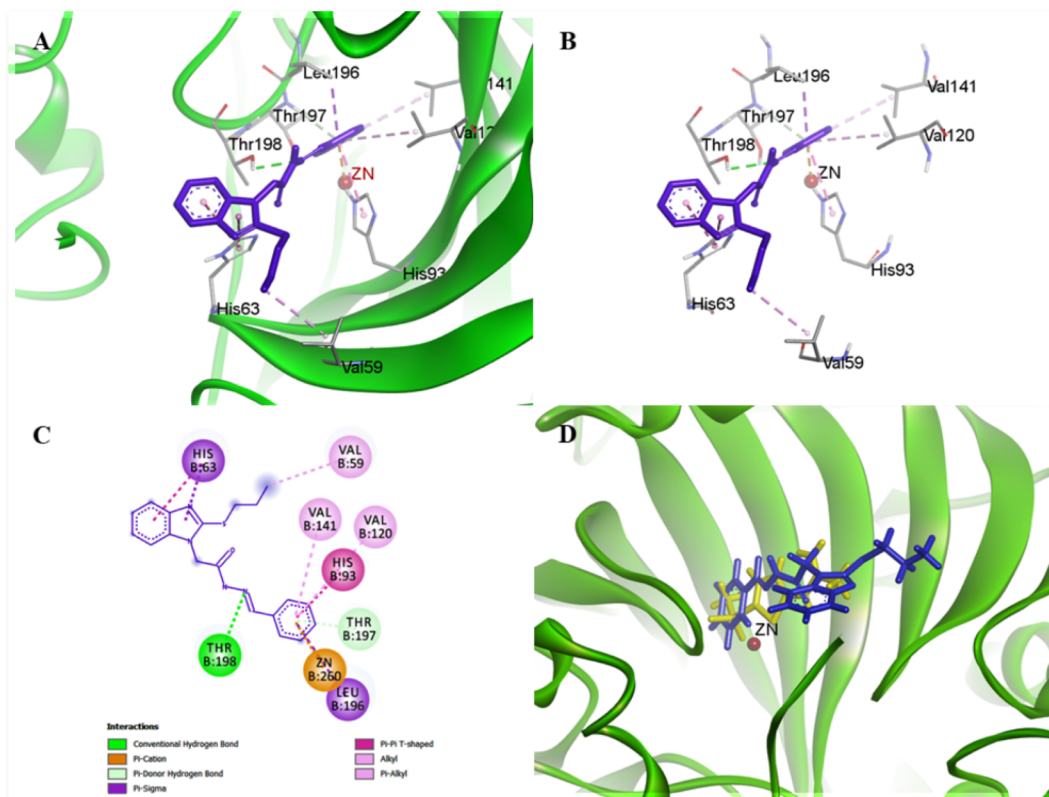
Figure 4. (A) Close-up view of the top-scoring pose of compound **10** (blue stick model) showing detailed ligand−enzyme interactions; (B) stereoview of ligand−enzyme interactions; (C) 2D view of ligand−enzyme interactions; and (D) compound **10** (blue stick model) superimposed on acetazolamide (yellow stick model), the active site.

Synthesis of 2-(2-(Propylthio)-1*H*-benzo[*d*]imidazol-1-yl)acetohydrazide (7). In an RB flask, 60 mmol ethyl-2-(2-(propylthio)benzimidazolyl)acetate (14.88 g) (**5**) was taken in methanol and stirred for 5 min. Then, 80 mmol (4 g, 4 mL) $N_2H_4 \cdot H_2O$ (**6**) was added and refluxed for 12 h. After completion, the mixture was decanted into distilled ice water to get the precipitated product (**7**). The product was filtered, washed with water, and dried. White amorphous solid, mp 95−97 °C (yield 82%). 1H NMR (600 MHz, DMSO): δ (ppm) = 7.12−7.53 m, (4H, Ar−H), 4.74 s, (2H, −NCH₂), 3.46−4.45 m, (3H, −CONHN$\underline{H_2}$), 0.95−3.30 m, (7H, SCH₂CH₂CH₃).

Synthesis of *N*-Acylhydrazones (9−29). The acetohydrazide (**7**) obtained in the previous step was refluxed for 3−4 h with different aldehydes (3 mmol) (**8**), which yielded the respective *N*-acylhydrazones (**9−29**). The reaction mixture was decanted into distilled cold water. The product precipitated was filtered, washed, and dried. The structures of all the compounds (**9−29**) were found consistent with their HR-MS(ESI), ¹H NMR, and ¹³C NMR spectra. Their spectral data and physical properties are given below.

N′-(2-Hydroxy-3-methoxybenzylidene)-2-(2-(propylthio)-1H-benzo[d]imidazol-1-yl)acetohydrazide (9). Amorphous solid; yield: 90%; mp 203−206 °C; ¹H NMR (600 MHz, DMSO, δ in ppm): δ (0.95−0.98) m, 3H, −CH₂−CH₂−C$\underline{H_3}$, (1.71) sextet, *J* = 7.2 Hz, 2H, −CH₂−C$\underline{H_2}$−CH₃, (3.24−3.28) m, 2H, −C$\underline{H_2}$−CH₂−CH₃, (3.82) s, 3H, Ar−OCH₃, (5.37) s, 2H, N−CH₂CO, (6.81−7.17) m, 4H, Ar−H, (7.40−7.55) m, 3H, Ar−H, (9.36) s, 1H, Ar−OH, (8.39) s, 1H, −N=CH, (11.73) s, 1H, −NHCO.
¹³C NMR (150 MHz, DMSO, δ in ppm): 167.31 (−C=O), 162.63 (−N=C−), 152.05 (Ar−C), 148.07 (Ar−C), 147.50

(=C−S), 146.07 (Ar−C), 137.02 (Ar−C), 121.71 (Ar−C), 121.58 (Ar−C), 120.55 (Ar−C), 119.23 (Ar−C), 118.97 (Ar−C), 117.65 (Ar−C), 113.94 (Ar−C), 109.80 (Ar−C), 55.95 (−OCH₃), 44.49 (−CH₂), 34.05 (−CH₂−), 22.51 (−CH₂−), 13.07 (−CH₃).
HR-MS (ESI) (*m/z*): [M + H]⁺ calcd for [C₂₀H₂₃N₄O₃S]⁺, 399.1485; found, 399.1472.

N′-Benzylidene-2-(2-(propylthio)-1H-benzo[d]imidazol-1-yl)acetohydrazide (10). Amorphous solid; yield; 91%; mp 220−223 °C; ¹H NMR (600 MHz, DMSO, δ in ppm): δ (0.95−0.98) m, 3H, −CH₂−CH₂−C$\underline{H_3}$, (1.68−1.74) m, 2H, −CH₂−C$\underline{H_2}$−CH₃, (3.26) t, *J* = 7.2 Hz, 2H, −C$\underline{H_2}$−CH₂−CH₃, (5.40) s, 2H, N−CH₂CO, (7.14−7.7.15) m, 2H, Ar−H, (7.43−7.56) m, 5H, Ar−H, (7.76−7.77) m, 2H, Ar−H, (8.06) s, 1H, −N=CH, (11.81) s, 1H, −CONH.
¹³C NMR (150 MHz, DMSO, δ in ppm): 167.62 (−C=O), 152.06 (−N=C−), 144.43 (=C−S), 142.92 (Ar−C), 137.01 (Ar−C), 133.95 (Ar−C), 130.14 (Ar−C), 128.87 (2Ar−C), 127.21 (Ar−C), 127.09 (Ar−C), 121.61 (Ar−C), 121.44 (Ar−C), 117.55 (Ar−C), 109.78 (Ar−C), 44.54 (−CH₂), 34.04 (−CH₂−), 22.51 (−CH₂−), 13.06 (−CH₃).
HR-MS (ESI) (*m/z*): [M + H]⁺ calcd for [C₁₉H₂₁N₄OS]⁺, 353.1431; found, 353.1418.

N′-(3-Methoxybenzylidene)-2-(2-(propylthio)-1H-benzo-[d]imidazol-1-yl)acetohydrazide (11). Amorphous solid; yield; 88%; mp 209−212 °C; ¹H NMR (600 MHz, DMSO, δ in ppm): δ (0.97−1.00) m, 3H, −CH₂−CH₂−C$\underline{H_3}$, (1.73) sextet, *J* = 7.2 Hz 2H, −CH₂−C$\underline{H_2}$−CH₃, (3.28) t, *J* = 7.2 Hz, 2H, −C$\underline{H_2}$−CH₂−CH₃, (3.81) s, 3H, Ar−OCH₃, (5.42) s, 2H, −CH₂CO, (7.02−7.57), 8H, Ar−H, (8.04) s, 1H, −N=CH, (11.84) s, 1H, −CONH.
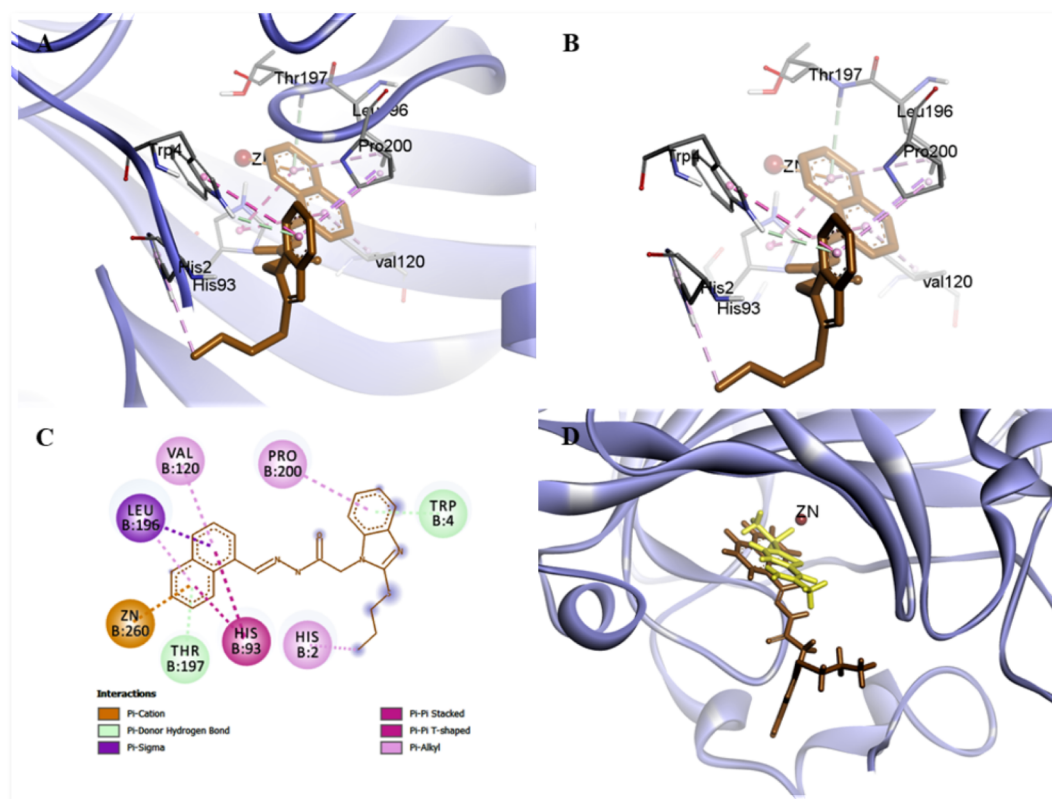
Figure 5. (A) Close-up view of the top-scoring pose of compound **12** (brown stick model) showing detailed ligand−enzyme interactions; (B) stereoview of ligand−enzyme interactions; (C) 2D view of ligand−enzyme interactions; and (D) compound **12** (brown stick model) superimposed on acetazolamide (yellow stick model), the active site.

^{13}C NMR (150 MHz, DMSO, δ in ppm): 169.80 (−C=O), 152.88 (−N=C−), 146.45 (Ar−C), 143.50 (=C−S), 137.50 (Ar−C), 135.60 (Ar−C), 130.50 (Ar−C), 128.20 (Ar−C), 122.10 (Ar−C), 121.90 (Ar−C), 118.80 (Ar−C), 117.80 (Ar−C), 111.50 (2Ar−C), 105.84 (Ar−C), 55.60 (−OCH$_3$), 44.53 (−CH$_2$), 35.12 (−CH$_2$−), 22.81 (−CH$_2$−), 13.34 (−CH$_3$).

HR-MS (ESI) (m/z): [M + H]$^+$ calcd for [C$_{20}$H$_{23}$N$_4$O$_2$S]$^+$, 383.1536; found, 383.1523.

N′-(Naphthalen-1-ylmethylene)-2-(2-(propylthio)-1H-benzo[d]imidazol-1-yl)acetohydrazide (12). Amorphous solid; yield; 85%; mp 217−220 °C; ^{1}H NMR (600 MHz, DMSO, δ in ppm): δ (0.97−1.01) m, 3H, −CH$_2$−CH$_2$−C<u>H</u>$_3$, (1.71−1.76) m, 2H, −CH$_2$−C<u>H</u>$_2$−CH$_3$, (3.27−3.30) m, 2H, −C<u>H</u>$_2$−CH$_2$−CH$_3$, (5.50) s, 2H, −CH$_2$CO, (7.17−8.07), 11H, Ar−<u>H</u>, (8.77) s, 1H, −N=CH, (11.89) s, 1H, −CONH.

^{13}C NMR (150 MHz, DMSO, δ in ppm): 168.89 (−C=O), 152.70 (−N=C−), 145.71 (=C−S−), 137.45 (Ar−C), 134.45 (Ar−C), 131.45 (2Ar−C), 128.20 (2Ar−C), 129.01 (Ar−C), 128.50 (Ar−C), 127.59 (Ar−C), 126.38 (Ar−C), 125.27 (Ar−C), 123.68 (3Ar−C), 118.56 (Ar−C), 108.60 (Ar−C), 44.19 (CH$_2$) 35.15 (−CH$_2$−), 22.81 (−CH$_2$−), 13.35 (−CH$_3$).

HR-MS (ESI) (m/z): [M + H]$^+$ calcd for [C$_{23}$H$_{23}$N$_4$OS]$^+$, 403.1587; found, 403.1573.

N′-(3,4-Dimethoxybenzylidene)-2-(2-(propylthio)-1H-benzo[d]imidazol-1-yl)acetohydrazide (13). Amorphous solid; yield; 90%; mp 180−183 °C; ^{1}H NMR (600 MHz, DMSO, δ in ppm): δ (0.95−0.98) m, 3H, −CH$_2$−CH$_2$−C<u>H</u>$_3$, (1.72) sextet J = 7.2 Hz, 2H, −CH$_2$−C<u>H</u>$_2$−CH$_3$, (3.24−3.28) m, 2H, −C<u>H</u>$_2$−CH$_2$−CH$_3$, (3.81) s, 3H, Ar−OCH$_3$, (3.85) s,

3H, Ar−OCH$_3$, (5.35) s, 2H, −CH$_2$CO, (6.59−7.85), 7H, Ar−H, (8.29) s, 1H, −N=CH, (11.61) s, 1H, −CONH.

^{13}C NMR (150 MHz, DMSO, δ in ppm): 167.18 (−C=O), 162.49 (−N=C−), 159.17 (Ar−C) 152.06 (Ar−C), 142.94 (=C−S−), 140.16 (Ar−C), 137.02 (Ar−C), 126.89 (Ar−C), 121.56 (2Ar−C), 117.63 (Ar−C), 114.82 (Ar−C), 109.77 (Ar−C), 106.56 (Ar−C), 98.35 (Ar−C), 55.86 (−OCH$_3$), 55.51 (−OCH$_3$), 44.58 (−CH$_2$), 34.08 (−CH$_2$−), 22.51 (−CH$_2$−), 13.06 (−CH$_3$).

HR-MS (ESI) (m/z): [M + H]$^+$ calcd for [C$_{21}$H$_{25}$N$_4$O$_3$S]$^+$, 413.1642; found, 413.1632.

N′-(2,4-Dihydroxybenzylidene)-2-(2-(propylthio)-1H-benzo[d]imidazol-1-yl)acetohydrazide (14). Amorphous solid; yield; 90%; mp 250−253 °C; ^{1}H NMR (600 MHz, DMSO, δ in ppm): δ (0.95−0.98) m, 3H, −CH$_2$−CH$_2$−C<u>H</u>$_3$, (1.67−1.75) m, 2H, −CH$_2$−C<u>H</u>$_2$−CH$_3$, (3.24−3.28) m, 2H, −C<u>H</u>$_2$−CH$_2$−CH$_3$, (5.32) s, 2H, −CH$_2$CO, (6.28−7.59), 7H, Ar−H, (9.98) s, 2H, Ar−OH; (8.23) s, 1H, −N=CH, (11.52) s, 1H, −NHCO.

^{13}C NMR (150 MHz, DMSO, δ in ppm): 166.79 (−C=O), 162.20 (Ar−C), 160.93 (Ar−C), 159.32 (−N=C−), 142.91 (=C−S−), 137.02, (Ar−C), 131.03 (Ar−C), 128.01 (Ar−C), 121.51 (2Ar−C), 117.64 (Ar−C), 111.63 (Ar−C), 109.79 (Ar−C), 107.92 (Ar−C), 102.61 (Ar−C), 45.02 (−CH$_2$), 34.07 (−CH$_2$), 22.51 (−CH$_2$−), 13.06 (−CH$_3$).

HR-MS (ESI) (m/z): [M + H]$^+$ calcd for [C$_{19}$H$_{21}$N$_4$O$_3$S]$^+$, 385.1329; found, 385.1318.

N′-(2,4-Dimethoxybenzylidene)-2-(2-(propylthio)-1H-benzo[d]imidazol-1-yl)acetohydrazide (15). Amorphous solid; yield; 91%; mp 186−189 °C; ^{1}H NMR (600 MHz, DMSO, δ in ppm): δ (0.95−0.99) m, 3H, −CH$_2$−CH$_2$−C<u>H</u>$_3$,
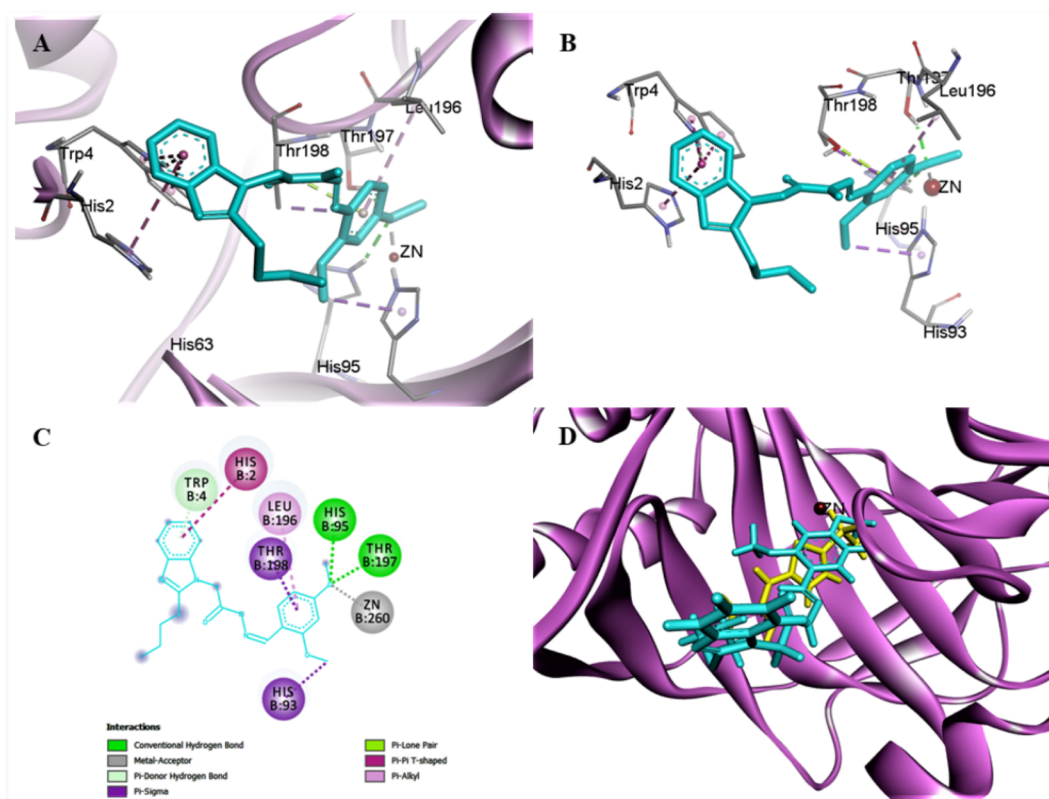
Figure 6. (A) Close-up view of the top-scoring pose of compound **15** (cyan stick model) showing detailed ligand−enzyme interactions; (B) stereoview of ligand−enzyme interactions; (C) 2D view of ligand−enzyme interactions; and (D) compound **15** (cyan stick model) superimposed on acetazolamide (yellow stick model), the active site.

(1.72) sextet, J = 7.2 Hz, 2H, −CH$_2$−C$\underline{H}_2$−CH$_3$, (3.25−3.28) m, 2H, −C$\underline{H}_2$−CH$_2$−CH$_3$, (3.80) s, 3H, Ar−OCH$_3$, (3.81) s, 3H, Ar−OCH$_3$, (5.40) s, 2H, −CH$_2$CO, (7.00−7.56), 7H, Ar−H, (7.98) s, 1H, −N═CH, (11.7) s, 1H, −CONH.

^{13}C NMR (150 MHz, DMSO, δ in ppm): 167.38 (−C═O), 152.10 (−N═C−), 149.12 (Ar−C), 144.48 (Ar−C) 142.88 (═C−S−), 136.99 (Ar−C), 131.65 (Ar−C), 126.70 (Ar−C), 121.60 (Ar−C), 121.52 (Ar−C), 121.45 (Ar−C), 117.53 (Ar−C), 111.61 (Ar−C), 109.79 (2Ar−C), 55.64 (−OCH$_3$), 55.61 (−OCH$_3$), 44.58 (−CH$_2$), 34.06 (−CH$_2$−), 22.51 (−CH$_2$−), 13.06 (−CH$_3$).

HR-MS (ESI) (m/z): [M + H]$^+$ calcd for [C$_{21}$H$_{25}$N$_4$O$_3$S]$^+$, 413.1642; found, 413.1614.

N′-(4-(Diethylamino)benzylidene)-2-(2-(propylthio)-1H-benzo[d]imidazol-1-yl)acetohydrazide (16). Amorphous solid; yield; 92%; mp 184−187 °C; ^{1}H NMR (600 MHz, DMSO, δ in ppm): δ (0.96) t, J = 7.1 Hz, 3H, −CH$_2$−CH$_2$−C$\underline{H}_3$, (1.10−1.12) m, 6H, Ar−N(CH$_2$−C$\underline{H}_3$)$_2$, (1.70−1.74) m, 2H, −CH$_2$−C$\underline{H}_2$−CH$_3$, (3.15−3.27) m, 6H, (−C$\underline{H}_2$−CH$_2$−CH$_3$ & Ar−N(C$\underline{H}_2$−CH$_3$)$_2$), (5.74) s, 2H, −CH$_2$CO, (6.68−7.55), 8H, Ar−H; (7.89) s, 1H, −N═CH, (11.47) s, 1H, −CONH.

^{13}C NMR (150 MHz, DMSO, δ in ppm): 167.69 (−C═O), 152.79 (−N═C−), 146.61 (Ar−C), 143.54 (═C−S) 139.50 (Ar−C), 136.66 (Ar−C), 129.13 (Ar−C), 122.12 (2Ar−C), 121.93 (2Ar−C), 119.90 (Ar−C), 118.44 (2Ar−C), 111.15 (Ar−C), 44.85 (−CH$_2$−), 44.48 (2N−CH$_2$−), 35.12 (−CH$_2$−), 22.82 (−CH$_2$−), 13.37 (−CH$_3$), 12.58 (2-CH$_3$).

HR-MS (ESI) (m/z): [M + H]$^+$ calcd for [C$_{23}$H$_{30}$N$_5$OS]$^+$, 424.2166; found, 424.2155.

N′-(3-Hydroxybenzylidene)-2-(2-(propylthio)-1H-benzo[d]imidazol-1-yl)acetohydrazide (17). Amorphous solid; yield; 90%; mp 211−214 °C; ^{1}H NMR (600 MHz, DMSO, δ in ppm): δ (0.95−0.98) m, 3H, −CH$_2$−CH$_2$−C$\underline{H}_3$, (1.70−1.73) m, 2H, −CH$_2$−C$\underline{H}_2$−CH$_3$, (3.25−3.28) m, 2H, −C$\underline{H}_2$−CH$_2$−CH$_3$, (5.38) s, 2H, −CH$_2$CO, (6.80−7.56), 8H, Ar−H, (7.93) s, 1H, −N═CH, (9.62) s, 1H. Ar−OH, (11.75) s, 1H, −NHCO.

^{13}C NMR (150 MHz, DMSO, δ in ppm): 167.50 (−C═O), 157.69 (−N═C−), 152.01 (Ar−C) 144.63 (═C−S−), 142.94 (Ar−C), 137.02 (Ar−C), 135.18 (Ar−C), 129.91 (Ar−C), 121.51 (Ar−C), 121.42 (Ar−C), 118.98 (Ar−C), 118.55 (Ar−C), 117.55 (Ar−C), 112.93 (Ar−C), 109.79 (Ar−C), 44.44 (−CH$_2$−), 34.04 (−CH$_2$−), 22.51 (−CH$_2$−), 13.06 (−CH$_3$).

HR-MS (ESI) (m/z): [M + H]$^+$ calcd for [C$_{19}$H$_{21}$N$_4$O$_2$S]$^+$, 369.1380; found, 369.1332.

N′-(4-Hydroxy-3-methoxybenzylidene)-2-(2-(propylthio)-1H-benzo[d]imidazol-1-yl)acetohydrazide (18). Amorphous solid; yield: 89%; mp 206−209 °C; ^{1}H NMR (600 MHz, DMSO, δ in ppm): δ (0.95−0.97) m, 3H, −CH$_2$−CH$_2$−C$\underline{H}_3$, (1.70−1.73) m, 2H, −CH$_2$−C$\underline{H}_2$−CH$_3$, (3.14−3.15) m, 2H, −C$\underline{H}_2$−CH$_2$−CH$_3$, (3.81) s, 3H, Ar−OCH$_3$, (5.75) s, 2H, −CH$_2$CO, (6.82−7.54), 7H, Ar−H, (7.95) s, 1H, −N═CH, (9.54) s, 1H, Ar−OH, (11.63) s, 1H, −CONH.

^{13}C NMR (150 MHz, DMSO, δ in ppm): 168.60 (−C═O), 152.60 (−N═C−), 151.70 (Ar−C), 150.30 (Ar−C), 147.30 (═C−S), 136.70 (Ar−C), 132.90 (Ar−C), 131.90 (Ar−C), 123.80 (2Ar−C), 122.70 (Ar−C), 117.80 (Ar−C), 116.90 (Ar−C), 114.20 (Ar−C), 110.20 (Ar−C), 56.80 (−OCH$_3$),

44.60 (−CH$_2$−), 35.18 (−CH$_2$−), 22.70 (−CH$_2$−), 13.35 (−CH$_3$).

HR-MS (ESI) (m/z): [M + H]$^+$ calcd for [C$_{20}$H$_{23}$N$_4$O$_3$S]$^+$, 399.1485; found, 399.1468.

N′-(4-Methylbenzylidene)-2-(2-(propylthio)-1H-benzo[d]-imidazol-1-yl)acetohydrazide (19). Amorphous solid; yield; 85%; mp 203−206 °C; ^{1}H NMR (600 MHz, DMSO, δ in ppm): δ (0.95−0.98) m, 3H, −CH$_2$−CH$_2$−C$\underline{H}_3$, (1.71) sextet, J = 7.2 Hz, 2H, −CH$_2$−C$\underline{H}_2$−CH$_3$, (2.34) s, 3H, Ar−CH$_3$, (3.24−3.28) m, 2H, −C$\underline{H}_2$−CH$_2$−CH$_3$, (5.38) s, 2H, −CH$_2$CO, (7.13−7.56), 8H, Ar−H, (8.02) s, 1H, −N═CH; (11.74) s, 1H, −CONH.

^{13}C NMR (150 MHz, DMSO, δ in ppm): 167.49 (−C═O), 152.05 (−N═C−), 144.50 (═C−S−), 142.95 (Ar−C), 139.95 (Ar−C), 137.02 (Ar−C), 131.25 (Ar−C), 129.46 (2Ar−C), 127.19 (Ar−C), 127.07 (Ar−C), 121.58 (Ar−C), 121.41 (Ar−C), 117.55 (Ar−C), 109.78 (Ar−C), 44.53 (−CH$_2$−), 34.04 (−CH$_2$−), 22.51 (−CH$_2$−), 21.07 (−CH$_3$), 13.06 (−CH$_3$).

HR-MS (ESI) (m/z): [M + H]$^+$ calcd for [C$_{20}$H$_{23}$N$_4$OS]$^+$, 367.1587; found, 367.1589.

N′-(3-Ethoxy-4-hydroxybenzylidene)-2-(2-(propylthio)-1H-benzo[d]imidazol-1-yl)acetohydrazide (20). Amorphous solid; yield: 88%; mp 222−225 °C; ^{1}H NMR (600 MHz, DMSO, δ in ppm): δ (0.95−0.98) m, 3H, −CH$_2$−CH$_2$−C$\underline{H}_3$, (1.34) t, J = 6.6 Hz, 3H, Ar−O−CH$_2$−C$\underline{H}_3$, (1.69−1.75) m, 2H, −CH$_2$−C$\underline{H}_2$−CH$_3$, (3.24−3.28) m, 2H, −C$\underline{H}_2$−CH$_2$−CH$_3$, (4.05) q, J = 6.6 Hz, 2H, Ar−O−C$\underline{H}_2$−CH$_3$, (5.37) s, 2H, −CH$_2$CO, (6.81−7.60), 7H, Ar−H, (7.92) s, 1H, −N═CH, (9.45) s, 1H, Ar−OH, (11.61) s, 1H, −CONH.

^{13}C NMR (150 MHz, DMSO, δ in ppm): 167.27 (−C═O), 159.13 (−N═C), 147.18 (Ar−C), 144.82 (Ar−C) 141.33 (═C−S−), 137.10 (Ar−C), 132.80 (Ar−C) 125.55 (Ar−C), 125.01 (Ar−C), 121.56 (Ar−C), 121.41 (Ar−C), 117.55 (Ar−C), 115.64 (Ar−C), 110.97 (Ar−C), 109.78 (Ar−C), 63.99 (−OCH$_2$−), 44.67 (−CH$_2$−), 35.10 (−CH$_2$), 22.51 (−CH$_2$−), 14.72 (−CH$_3$), 13.06 (−CH$_3$).

HR-MS (ESI) (m/z): [M + H]$^+$ calcd for [C$_{21}$H$_{25}$N$_4$O$_3$S]$^+$, 413.1642; found, 413.1625.

N′-(4-Formylbenzylidene)-2-(2-(propylthio)-1H-benzo[d]-imidazol-1-yl)acetohydrazide (21). Amorphous solid; yield; 90%; mp 282−285 °C; ^{1}H NMR (600 MHz, DMSO, δ in ppm): δ (0.96) t, J = 7.2 Hz, 3H, −CH$_2$−CH$_2$−C$\underline{H}_3$, (1.70−1.74) m, 2H, −CH$_2$−C$\underline{H}_2$−CH$_3$, (3.26) t, J = 7.2 Hz, 2H, −C$\underline{H}_2$−CH$_2$−CH$_3$, (5.42) s, 2H, −CH$_2$CO, (7.15−8.00), 8H, Ar−H, (8.07) s, 1H, −N═CH, (10.04) s, 1H, Ar−CHO, (11.82) s, 1H, −CONH.

^{13}C NMR (150 MHz, DMSO, δ in ppm): 192.47 (−CHO), 167.63 (−C═O), 152.06 (−N═C), 150.20 (Ar−C), 142.94 (═C−S), 137.01 (Ar−C), 132.01 (Ar−C), 129.94 (Ar−C), 127.66 (Ar−C), 127.04 (Ar−C), 126.92 (2Ar−C), 121.61 (Ar−C), 121,44 (Ar−C), 117.56 (Ar−C), 109.78 (Ar−C), 44.55 (−CH$_2$−), 34.04 (−CH$_2$−), 22.51 (−CH$_2$−), 13.06 (−CH$_3$).

HR-MS (ESI) (m/z): [M + H]$^+$ calcd for [C$_{20}$H$_{21}$N$_4$O$_2$S]$^+$, 381.1380; found, 381.1381.

N′-(4-Isopropylbenzylidene)-2-(2-(propylthio)-1H-benzo-[d]imidazol-1-yl)acetohydrazide (22). Amorphous solid; yield; 88%; mp 180−183 °C; ^{1}H NMR (600 MHz, DMSO, δ in ppm): δ (0.95−0.98) m, 3H, −CH$_2$−CH$_2$−C$\underline{H}_3$, (1.19−1.21) m, 6H, −CH(C$\underline{H}_3$)$_2$, (1.71) sextet, J = 7.2 Hz, 2H, −CH$_2$−C$\underline{H}_2$−CH$_3$, (3.24−3.28) m, 2H, −C$\underline{H}_2$−CH$_2$−CH$_3$, (3.91−3.94) m, 1H, −C$\underline{H}$(CH$_3$)$_2$, (5.38) s, 2H, −CH$_2$CO,

(7.13−7.68), 8H, Ar−H, (8.02) s, 1H, −N═CH, (11.75) s, 1H, −CONH.

^{13}C NMR (150 MHz, DMSO, δ in ppm): 167.50 (−C═O), 152.04 (−N═C), 150.10 (Ar−C), 143.50 (═C−S−), 143.00 (Ar−C), 137.01 (Ar−C), 131.66 (Ar−C), 127.18 (Ar−C), 126.82 (Ar−C), 121.59 (Ar−C), 121.42 (Ar−C), 117.57 (2Ar−C), 109.77 (Ar−C), 108.62 (Ar−C),56.31 (−CH−), 44.80 (−CH$_2$−), 35.12 (−CH$_2$−), 22.83 (−CH$_2$−), 15.30 (2CH$_3$), 13.34 (−CH$_3$).

HR-MS (ESI) (m/z): [M + H]$^+$ calcd for [C$_{22}$H$_{27}$N$_4$OS]$^+$, 395.1900; found, 395.1889.

2-(2-(Propylthio)-1H-benzo[d]imidazol-1-yl)-N′-(thio-phen-2-ylmethylene)acetohydrazide (23). Amorphous solid; yield; 90%; mp 188−191 °C; ^{1}H NMR (600 MHz, DMSO, δ in ppm): δ (0.95−0.98) m, 3H, −CH$_2$−CH$_2$−C$\underline{H}_3$, (1.68−1.75) m, 2H, −CH$_2$−C$\underline{H}_2$−CH$_3$, (3.24−3.28) m, 2H, −C$\underline{H}_2$−CH$_2$−CH$_3$, (5.30) s, 2H, −CH$_2$CO, (7.13−7.67), 7H, Ar−H, (8.24) s, 1H, −N═CH, (11.78) s, 1H, −CONH.

^{13}C NMR (150 MHz, DMSO, δ in ppm): 167.21 (−C═O), 151.49 (−N═C−), 143.93 (Ar−C), 139.60 (═C−S), 137.02 (Ar−C), 131.63 (Ar−C), 129.22 (2Ar−C), 128.43 (Ar−C), 121.59 (Ar−C), 121.42 (Ar−C), 117.57 (Ar−C), 109.77 (Ar−C), 45.13 (−CH$_2$−) 34.07 (−CH$_2$−), 22.50 (−CH$_2$−), 13.05 (−CH$_3$).

HR-MS (ESI) (m/z): [M + H]$^+$ calcd for [C$_{17}$H$_{19}$N$_4$OS$_2$]$^+$, 359.0995; found, 359.0987.

N′-(4-Fluorobenzylidene)-2-(2-(propylthio)-1H-benzo[d]-imidazol-1-yl)acetohydrazide (24). Amorphous solid; yield; 88%; mp 204−207 °C; ^{1}H NMR (600 MHz, DMSO, δ in ppm): δ (0.95−0.98) m, 3H, −CH$_2$−CH$_2$−C$\underline{H}_3$, (1.72) sextet, J = 7.0 Hz, 2H, −CH$_2$−C$\underline{H}_2$−CH$_3$, (3.24−3.28) m, 2H, −C$\underline{H}_2$−CH$_2$−CH$_3$, (5.40) s, 2H, −CH$_2$CO, (7.12−7.84), 8H, Ar−H, (8.05) s, 1H, −N═CH, (11.81) s, 1H, −NHCO.

^{13}C NMR (150 MHz, DMSO, δ in ppm): 167.63 (−C═O), 163.75 (Ar−C) 152.07 (−N═C) 144.95 (═S−C), 143.27 (Ar−C) 137.01 (Ar−C), 130.61 (Ar−C), 129.34 (Ar−C), 129.29 (Ar−C), 121.59 (Ar−C), 121.42 (Ar−C), 117.56 (Ar−C), 115.98 (Ar−C), 115.83 (Ar−C), 109.75 (Ar−C), 44.54 (−CH$_2$−), 34.04 (−CH$_2$−), 22.51 (CH$_2$−), 13.05 (−CH$_3$).

HR-MS (ESI) (m/z): [M + H]$^+$ calcd for [C$_{19}$H$_{20}$FN$_4$OS]$^+$, 371.1336; found, 371.1300.

N′-(Furan-2-ylmethylene)-2-(2-(propylthio)-1H-benzo[d]-imidazol-1-yl)acetohydrazide (25). Amorphous solid; yield: 89%; mp 170−173 °C; ^{1}H NMR (600 MHz, DMSO, δ in ppm): δ (0.96) t, J = 7.2 Hz, 3H, −CH$_2$−CH$_2$−C$\underline{H}_3$, (1.71) sextet, J = 7.2 Hz, 2H, −CH$_2$−C$\underline{H}_2$−CH$_3$, (3.26) t, J = 7.2 Hz, 2H, −C$\underline{H}_2$−CH$_2$−CH$_3$, (5.31) s, 2H, −CH$_2$CO, (6.63−7.85), 7H, Ar−H, (7.94) s, 1H, −N═CH, (11.76) s, 1H, −CONH.

^{13}C NMR (150 MHz, DMSO, δ in ppm): 167.54 (−C═O), 154.54 (−N═C), 149.34 (Ar−C), 143.49 (Ar−C), 141.32 (═C−S), 136.55 (Ar−C), 134.55 (Ar−C), 122.18 (Ar−C), 121.61 (Ar−C), 117.52 (Ar−C), 112.25 (Ar−C), 109.83 (2Ar−C), 44.37 (−CH$_2$−), 34.07 (−CH$_2$−), 22.50 (−CH$_2$−), 13.05 (−CH$_3$).

HR-MS (ESI) (m/z): [M + H]$^+$ calcd for [C$_{17}$H$_{19}$N$_4$O$_2$S]$^+$, 343.1223; found, 343.1202.

N′-((5-Methylfuran-2-yl)methylene)-2-(2-(propylthio)-1H-benzo[d]imidazol-1-yl)acetohydrazide (26). Amorphous solid; yield: 88%; mp 151−154 °C; ^{1}H NMR (600 MHz, DMSO, δ in ppm): δ (0.97) t, J = 7.2 Hz, 3H, −CH$_2$−CH$_2$−C$\underline{H}_3$, (1.22) s, 3H, Ar−CH$_3$, (1.69−1.73) m, 2H, −CH$_2$−C$\underline{H}_2$−CH$_3$, (3.23−3.26) m, 2H, −C$\underline{H}_2$−CH$_2$−CH$_3$, (5.28) s,

2H, −CH$_2$CO, (7.12−7.54), 6H, Ar−H, (7.90) s, 1H, −N═CH, (11.71) s, 1H, −CONH.

^{13}C NMR (150 MHz, DMSO, δ in ppm): 167.45 (−C═O), 155.98 (−N═C), 153.32 (Ar−C), 148.88 (Ar−C), 142.06 (═C−S), 137.43 (Ar−C), 133.15 (Ar−C), 122.01 (Ar−C), 120.89 (Ar−C), 116.57 (Ar−C), 111.11 (Ar−C), 108.63 (Ar−C), 108.30 (Ar−C), 44.53 (−CH$_2$−), 35.11 (−CH$_2$), 22.50 (−CH$_2$−) 13.91 (−CH$_3$), 13.05 (−CH$_3$).

HR-MS (ESI) (m/z): [M + H]$^+$ calcd for [C$_{18}$H$_{21}$N$_4$O$_2$S]$^+$, 357.1380; found, 357.1367.

N′-(2,3-Dimethoxybenzylidene)-2-(2-(propylthio)-1H-benzo[d]imidazol-1-yl)acetohydrazide (27). Amorphous solid; yield; 89%; mp 213−216 °C; ^{1}H NMR (600 MHz, DMSO, δ in ppm): δ (0.95−0.98) m, 3H, −CH$_2$−CH$_2$−C**H**$_3$, (1.71) sextet, 6.6 Hz, 2H, −CH$_2$−C**H**$_2$−CH$_3$, (3.24−3.28) m, 2H, −C**H**$_2$−CH$_2$−CH$_3$, (3.77) s, 3H, Ar−OCH$_3$, (3.83) s, 3H, Ar−OCH$_3$, (5.38) s, 2H, −CH$_2$CO, (7.11−7.55), 7H, Ar−H, (8.34) s, 1H, −N═CH, (11.77) s, 1H, −CONH.

^{13}C NMR (150 MHz, DMSO, δ in ppm): 167.52 (−C═O), 153.70 (−N═C), 152.05 (Ar−C), 148.04 (Ar−C), 143.51 (═C−S), 140.22 (Ar−C), 137.01 (Ar−C), 128.69 (Ar−C), 127.37 (Ar−C), 124.40 (Ar−C), 122.51 (Ar−C), 117.37 (Ar−C), 114.36 (Ar−C), 112.87 (Ar−C), 109.77 (Ar−C), 61.26 (−OCH$_3$), 55.84 (−OCH$_3$), 44.54 (−CH$_2$−), 34.03 (−CH$_2$−), 22.51 (−CH$_2$−), 13.06 (−CH$_3$).

HR-MS (ESI) (m/z): [M + H]$^+$ calcd for [C$_{21}$H$_{25}$N$_4$O$_3$S]$^+$, 413.1642; found, 413.1637.

N′-(2,6-Dichlorobenzylidene)-2-(2-(propylthio)-1H-benzo-[d]imidazol-1-yl)acetohydrazide (28). Amorphous solid; yield; 86%; mp 221−224 °C; ^{1}H NMR (600 MHz, DMSO, δ in ppm): (0.90−1.00) m, 3H, −CH$_2$−CH$_2$−C**H**$_3$, (1.70−1.74) m, 2H, −CH$_2$−C**H**$_2$−CH$_3$, (3.25−3.29) m, 2H, −C**H**$_2$−CH$_2$−CH$_3$, (5.76) s, 2H, −CH$_2$CO, (7.16−7.62), 7H, Ar−H, (8.33) s, 1H, −N═CH, (12.09) s, 1H, −NHCO.

^{13}C NMR (150 MHz, DMSO, δ in ppm): 168.50 (−C═O) 152.40 (−N═C), 143.15 (═C−S−), 140.10 (2Ar−C), 135.90 (Ar−C), 134.80 (Ar−C), 132.90 (Ar−C), 131.50 (2Ar−C), 130.8 (Ar−C), 122.50 (2Ar−C), 117.80 (Ar−C), 110.50 (Ar−C), 44.80 (−CH$_2$−), 35.10 (−CH$_2$−), 22.80 (−CH$_2$−), 13.30 (−CH$_3$).

HR-MS (ESI) (m/z): [M + H]$^+$ calcd for [C$_{19}$H$_{19}$Cl$_2$N$_4$OS]$^+$, 421.0651; found, 421.0569.

N′-(2-Methoxybenzylidene)-2-(2-(propylthio)-1H-benzo-[d]imidazol-1-yl)acetohydrazide (29). Amorphous solid; yield; 89%; mp 141−144 °C; ^{1}H NMR (600 MHz, DMSO, δ in ppm): (0.95−0.98) m, 3H, −CH$_2$−CH$_2$−C**H**$_3$, (1.69−1.73) m, 2H, −CH$_2$−C**H**$_2$−CH$_3$, (3.25) t, J = 7.2 Hz, 2H, −C**H**$_2$−CH$_2$−CH$_3$, (3.85) s, 3H, Ar−OCH$_3$, (5.38) s, 2H, −CH$_2$CO, (6.99−7.93), 8H, Ar−H, (8.39) s, 1H, −N═CH, (11.75) s, 1H, −NHCO.

^{13}C NMR (150 MHz, DMSO, δ in ppm): 167.06 (−C═O), 162.44 (−N═C), 151.93 (Ar−C), 142.81 (═C−S−), 137.01 (Ar−C), 131.77 (Ar−C), 131.23 (2Ar−C), 126.43 (2Ar−C), 122.41 (Ar−C), 121.63 (Ar−C), 121.43 (Ar−C), 117.54 (Ar−C), 109.81 (Ar−C), 55.80 (−OCH$_3$), 44.16 (−CH$_2$−), 35.10 (−CH$_2$−), 22.50 (−CH$_2$−), 13.05 (−CH$_3$).

HR-MS (ESI) (m/z): [M + H]$^+$ calcd for [C$_{20}$H$_{23}$N$_4$O$_2$S]$^+$, 383.1536; found, 383.1533.

Carbonic Anhydrase Inhibition Activity. In this assay, colorless 4-nitrophenyl acetate (4-NPA) is hydrolyzed to yellow 4-nitrophenol.[23] The assay was carried out at 25 °C in 20 mM HEPES-tris buffer of pH 7.4 in a 96-well plate. Each well of the 96-well plate comprised 140 μL of HEPES-tris buffer solution, 20 μL of fresh enzyme solution (0.1 mg/mL in buffer) of purified bovine erythrocyte CA II, and 20 μL of the test compound in DMSO (10% final concentration). The mixture of the enzyme and inhibitor was pre-incubated for 15 min at room temperature to allow the formation of the EI complex. After incubation, the reaction was initiated by adding 20 μL of substrate 4-NPA (0.7 mM). For kinetic studies, 0.8, 0.4, 0.2, and 0.1 mM substrate was used. It was followed by continuous measurement of the amount of the product formed at λ = 400 nm for 30 min at 1 min intervals in 96-well flat-bottom plates, using an ELISA Reader x MARK Microplate spectrophotometer, BIORAD (USA). The activity of control (in the absence of the inhibitor) was taken as 100%. The measurements were taken in triplicate at each used concentration.[21]

The % inhibition was calculated using the following formula

$$\% \text{ Inhibition} = 100 - (\text{OD test well}/\text{OD control}) \times 100$$

Molecular Docking. Two-dimensional (2D) structures of compounds 9−29 were drawn in ChemDraw and then altered to 3D structures, which were then minimized using Chimera. Docking simulations were carried out using GOLD software. For ligand molecules, the GOLD score was selected as a fitness function.[24] Different docking poses were made/generated using the GOLD program, and for each compound, the best-docked pose was selected, which is based on two criteria: (i) fitness function scores and (ii) the binding position of the ligand.[25] Carbonic anhydrase-II (PDB ID: 1V9E) was used as receptor proteins. The PDB structure was taken from the Protein Data Bank and updated, arranged using the GOLD program by carrying out different steps, that is, optimization of hydrogen bonds by flipping amino side chains, the addition of hydrogens, minimization of the protein complex, charge correction, and assigning of bond orders. All the ligands (bound), H$_2$O molecules, and cofactors were excluded from the proteins.[26] The interactions of synthesized docked compounds with various amino acids can be seen inside the selected binding pocket. Discovery Studio Visualizer software for visualization of 2D and 3D structures was used, and then, they were processed.

■ CONCLUSIONS

In conclusion, we were able to synthesize a new series of non-sulfonamide acylhydrazones and to test the new products for their potential against carbonic anhydrase enzyme. The in vitro carbonic anhydrase-II inhibition potential of the compounds displayed excellent results. Among the synthesized compounds, 9, 10, 12, and 15 showed the highest inhibition, even greater than that of the standard acetazolamide. The molecular docking results indicated a competitive inhibiting behavior of the synthesized compounds by recording metal−acceptor and π−cation interactions with Zn^{2+} ions. These findings are interesting in that non-sulfonamide compounds might also be considered in the drug development process against carbonic anhydrases.

■ AUTHOR INFORMATION

Corresponding Authors

Muhammad Saadiq − *Institute of Chemical Sciences, University of Peshawar, Peshawar, Khyber Pakhtunkhwa 25120, Pakistan;* ⦿ orcid.org/0000-0002-4963-4341; Email: saadiq@bkuc.edu.pk

Ghias Uddin − *Institute of Chemical Sciences, University of Peshawar, Peshawar, Khyber Pakhtunkhwa 25120, Pakistan*; Email: ghiasuddin@upesh.edu.pk

Authors

Abdul Latif − *Department of Chemistry, University of Malakand, Dir (Lower), Chakdara, Khyber Pakhtunkhwa 18800, Pakistan*

Mumtaz Ali − *Department of Chemistry, University of Malakand, Dir (Lower), Chakdara, Khyber Pakhtunkhwa 18800, Pakistan*

Nazia Akbar − *Department of Biotechnology & Genetic Engineering, Hazara University, Mansehra, Khyber Pakhtunkhwa 21120, Pakistan*

Ammara − *Department of Chemistry, University of Malakand, Dir (Lower), Chakdara, Khyber Pakhtunkhwa 18800, Pakistan*

Sardar Ali − *Department of Chemistry, University of Malakand, Dir (Lower), Chakdara, Khyber Pakhtunkhwa 18800, Pakistan*

Manzoor Ahmad − *Department of Chemistry, University of Malakand, Dir (Lower), Chakdara, Khyber Pakhtunkhwa 18800, Pakistan*; orcid.org/0000-0001-9736-5900

Mohammad Zahoor − *Department of Biochemistry, University of Malakand, Dir (Lower), Chakdara, Khyber Pakhtunkhwa 18800, Pakistan*

Ajmal Khan − *UoN Chair of Oman's Medicinal Plants and Marine Natural Products, University of Nizwa, Nizwa 616, Sultanate of Oman*

Ahmed Al-Harrasi − *UoN Chair of Oman's Medicinal Plants and Marine Natural Products, University of Nizwa, Nizwa 616, Sultanate of Oman*; orcid.org/0000-0002-0815-5942

Complete contact information is available at:
https://pubs.acs.org/10.1021/acsomega.1c05362

Notes

The authors declare no competing financial interest.

■ REFERENCES

(1) Bozdag, M.; Supuran, C. T.; Esposito, D.; Angeli, A.; Carta, F.; Monti, S. M.; De Simone, G.; Alterio, V. 2-Mercaptobenzoxazoles: a class of carbonic anhydrase inhibitors with a novel binding mode to the enzyme active site. *Chem. Commun.* **2020**, *56*, 8297−8300.

(2) Milite, C.; Amendola, G.; Nocentini, A.; Bua, S.; Cipriano, A.; Barresi, E.; Feoli, A.; Novellino, E.; Da Settimo, F.; Supuran, C. T.; Castellano, S.; Cosconati, S.; Taliani, S. Novel 2-substituted-benzimidazole-6-sulfonamides as carbonic anhydrase inhibitors: synthesis, biological evaluation against isoforms I, II, IX and XII and molecular docking studies. *J. Enzyme Inhib. Med. Chem.* **2019**, *34*, 1697−1710.

(3) Hou, Z.; Li, C.; Liu, Y.; Zhang, M.; Wang, Y.; Fan, Z.; Guo, C.; Lin, B.; Liu, Y. Design, synthesis and biological evaluation of carbohydrate-based sulphonamide derivatives as topical antiglaucoma agents through selective inhibition of carbonic anhydrase II. *J. Enzyme Inhib. Med. Chem.* **2020**, *35*, 383−390.

(4) Pala, N.; Micheletto, L.; Sechi, M.; Aggarwal, M.; Carta, F.; McKenna, R.; Supuran, C. T. Carbonic anhydrase inhibition with benzenesulfonamides and tetrafluorobenzenesulfonamides obtained via click chemistry. *ACS Med. Chem. Lett.* **2014**, *5*, 927−930.

(5) Lomelino, C.; Supuran, C.; McKenna, R. Non-Classical Inhibition of Carbonic Anhydrase. *Int. J. Mol. Sci.* **2016**, *17*, 1150.

(6) Akhtar, W.; Khan, M. F.; Verma, G.; Shaquiquzzaman, M.; Rizvi, M. A.; Mehdi, S. H.; Akhter, M.; Alam, M. M. Therapeutic evolution of benzimidazole derivatives in the last quinquennial period. *Eur. J. Med. Chem.* **2017**, *126*, 705−753.

(7) Kalinina, T.S.; Shimshirt, A.A.; Volkova, A.V.; Korolev, A.O.; Voronina, T.A. Anxiolytic effects of diazepam and afobazole on the anxiety response evoked by gaba (a) receptor blockade in wistar rats and inbred mice of balb/c and c57bi/6 strains. *Eksp. Klin. Farmakol.* **2016**, *79*, 3−7.

(8) Bischof, J.; Leban, J.; Zaja, M.; Grothey, A.; Radunsky, B.; Othersen, O.; Strobl, S.; Vitt, D.; Knippschild, U. 2-Benzamido-N-(1H-benzo [d] imidazol-2-yl) thiazole-4-carboxamide derivatives as potent inhibitors of CK1δ/ε. *Amino Acids* **2012**, *43*, 1577−1591.

(9) Subramanian, S.; Costales, A.; Williams, T. E.; Levine, B.; McBride, C. M.; Poon, D.; Amiri, P.; Renhowe, P. A.; Shafer, C. M.; Stuart, D.; Verhagen, J.; Ramurthy, S. Design and synthesis of orally bioavailable benzimidazole reverse amides as pan RAF kinase inhibitors. *ACS Med. Chem. Lett.* **2014**, *5*, 989−992.

(10) Yadav, S.; Narasimhan, B.; Lim, S. M.; Ramasamy, K.; Vasudevan, M.; Shah, S. A. A.; Selvaraj, M. Synthesis, characterization, biological evaluation and molecular docking studies of 2-(1H-benzo [d] imidazol-2-ylthio)-N-(substituted 4-oxothiazolidin-3-yl) acet-amides. *Chem. Cent. J.* **2017**, *11*, 137.

(11) Anandarajagopal, K.; Tiwari, R. N.; Bothara, K.; Sunilson, J. A. J.; Dineshkumar, C.; Promwichit, P. 2-Mercaptobenzimidazole derivatives: synthesis and anticonvulsant activity. *Adv. Appl. Sci. Res.* **2010**, *1*, 132−138.

(12) Tahlan, S.; Kumar, S.; Ramasamy, K.; Lim, S. M.; Shah, S. A. A.; Mani, V.; Pathania, R.; Narasimhan, B. Design, synthesis and biological profile of heterocyclic benzimidazole analogues as prospective antimicrobial and antiproliferative agents. *BMC Chem.* **2019**, *13*, 50.

(13) Amer Hamada, H.; M. Ali, O.; El-Kafaween, I. K. Synthesis of some new nucleosides derived from 2-mercapto benzimidazole with expected biological activity. *Orient. J. Chem.* **2017**, *33*, 2303−2310.

(14) Alkhafaji, A.; Muhi-Eldeen, Z.; Al-Kaissi, E.; Al-Muhtaseb, N.; Arafat, T.; Ghattas, M. A. Synthesis, structural elucidation, and evaluation of antimicrobial activity of 5-ethoxy-2-mercaptobenzimi-dazole derivatives. *Int. j. med.* **2018**, *7*, 117−127.

(15) Keri, R. S.; Hiremathad, A.; Budagumpi, S.; Nagaraja, B. M. Comprehensive review in current developments of benzimidazole-based medicinal chemistry. *Chem. Biol. Drug Des.* **2015**, *86*, 19−65.

(16) Nevade, S. A.; Lokapure, S. G.; Kalyane, N. V. Synthesis and pharmacological evaluation of some novel 2-mercapto benzimidazole derivatives. *J. Korean Chem. Soc.* **2013**, *57*, 755−760.

(17) Syunyakov, T. S.; Neznamov, G. G. Evaluation of the therapeutic efficacy and safety of the selective anxiolytic afobazole in generalized anxiety disorder and adjustment disorders: Results of a multicenter randomized comparative study of diazepam. *Ter. Arkh.* **2016**, *88*, 73−86.

(18) Aboul-Enein, H. Y.; El Rashedy, A. Benzimidazole derivatives as antidiabetic agents. *Med. Chem.* **2015**, *5*, 318−325.

(19) Ali, M.; Ali, S.; Khan, M.; Rashid, U.; Ahmad, M.; Khan, A.; Al-Harrasi, A.; Ullah, F.; Latif, A. Synthesis, biological activities, and molecular docking studies of 2-mercaptobenzimidazole based derivatives. *Bioorg. Chem.* **2018**, *80*, 472−479.

(20) Latif, A.; Bibi, S.; Ali, S.; Ammara, A.; Ahmad, M.; Khan, A.; Al-Harrasi, A.; Ullah, F.; Ali, M. New multitarget directed benzimidazole-2-thiol-based heterocycles as prospective anti-radical and anti-Alzheimer's agents. *Drug Dev. Res.* **2021**, *82*, 207−216.

(21) Khan, A.; Khan, M.; Halim, S. A.; Khan, Z. A.; Shafiq, Z.; Al-Harrasi, A. Quinazolinones as competitive inhibitors of carbonic anhydrase-II (human and bovine): synthesis, in-vitro, in-silico, selectivity, and kinetics studies. *Front. Chem.* **2020**, *8*, 1−13.

(22) Saleem, M.; Saeed, A.; Atia-tul-Wahab; Khan, A.; Abbasi, S.; Khan, W.; Khan, S. B.; Choudhary, M. I. Benzamide sulfonamide derivatives: potent inhibitors of carbonic anhydrase-II. *Med. Chem. Res.* **2016**, *25*, 438−448.

(23) Pocker, Y.; Meany, J. E. The Catalytic Versatility of Erythrocyte Carbonic Anhydrase. II. Kinetic Studies of the Enzyme-Catalyzed Hydration of Pyridine Aldehydes. *Biochem* **1967**, *6*, 239−246.

(24) Verdonk, M. L.; Cole, J. C.; Hartshorn, M. J.; Murray, C. W.; Taylor, R. D. Improved protein−ligand docking using GOLD. *Proteins: Struct., Funct., Bioinf.* **2003**, *52*, 609−623.

(25) Politi, A.; Durdagi, S.; Moutevelis-Minakakis, P.; Kokotos, G.; Mavromoustakos, T. Development of accurate binding affinity predictions of novel renin inhibitors through molecular docking studies. *J. Mol. Graphics Modell.* **2010**, *29*, 425−435.

(26) Annamala, M. K.; Inampudi, K. K.; Guruprasad, L. Docking of phosphonate and trehalose analog inhibitors into M. tuberculosis mycolyltransferase Ag85C: Comparison of the two scoring fitness functions GoldScore and ChemScore, in the GOLD software. *Bioinformation* **2007**, *1*, 339−350.